Nonlinear giant magnetoimpedance and the asymmetric circumferential magnetization process in soft magnetic wires

2004 J. Phys.: Condens. Matter 16 5083

(http://iopscience.iop.org/0953-8984/16/28/026)

INSTITUTE OF PHYSICS PUBLISHING JOURNAL OF PHYSICS: CONDENSED MATTER

J. Phys.: Condens. Matter **16** (2004) 5083–5094 PII: S0953-8984(04)80674-X

Nonlinear giant magnetoimpedance and the asymmetric circumferential magnetization process in soft magnetic wires

C Gómez-Polo[1], J G S Duque[2] and M Knobel[2]

[1] Departamento de Física, Universidad Pública de Navarra, Campus de Arrosadía, 31006 Pamplona, Spain
[2] Instituto de Física 'Gleb Wataghin'(IFGW), Universidade Estadual de Campinas (UNICAMP), CP 6165, 13.083-970, Campinas, Sao Paulo, Brazil

Received 6 May 2004
Published 2 July 2004
Online at stacks.iop.org/JPhysCM/16/5083
doi:10.1088/0953-8984/16/28/026

Abstract

The magnetoimpedance effect and its nonlinear terms are analysed for a $(Co_{0.94}Fe_{0.06})_{72.5}Si_{12.5}B_{15}$ amorphous wire. In order to enhance the nonlinear contribution the sample was previously subjected to current annealing (Joule heating) to induce a circumferential anisotropy. The effect of the application of a torsional strain on the nonlinear magnetoimpedance is analysed in terms of the torsional dependence of the magnetic permeability, evaluated through experimental circumferential hysteresis loops. The results obtained clearly confirm the direct correlation between the asymmetric circumferential magnetization process and the occurrence of nonlinear second-harmonic terms in the magnetoimpedance voltage.

1. Introduction

The giant magnetoimpedance (GMI) effect, extensively studied during the last few decades, is one of the most promising magnetotransport effects owing to its direct application in highly sensitive magnetic and magnetoelastic sensors [1, 2]. The GMI consists of huge variations in the high frequency impedance that take place in a high permeability material upon the application of an external dc field, H [3]. GMI has been analysed in a wide variety of soft magnetic systems (amorphous and nanocrystalline wires, microwires, ribbons and thin films) [3].

Generally speaking, when an ac current, $I = I_0 e^{-i2\pi f t}$, flows through a soft magnetic sample, the associated transverse magnetic field magnetizes it, giving rise, for high enough current frequencies, to the so-called skin effect, where I remains mainly concentrated in a reduced region close to the sample surface. Under these circumstances, the complex impedance, $Z = R + iX$, is mainly determined by the associated magnetic permeability

which can be strongly changed by the application of different external agents, such as external magnetic fields and mechanical stresses. In particular, different works have recently been devoted to the analysis of the effect of a helical magnetoelastic anisotropy (application of torsional stress) on the GMI [4–8]. In these works, the torsional dependence of $Z(H)$ is mainly employed as a research tool in the study of the intrinsic magnetic anisotropies within the sample (i.e. quenched-in helical magnetoelastic anisotropy in amorphous wires). Beside this, the occurrence of an asymmetrical giant magnetoimpedance (AGMI) [9] in samples with helical anisotropy has reinforced the interest in these studies from a technological point of view. On the basis of the AGMI effect, new magnetic sensors are designed with improved reliability and linear characteristics [10].

On the other hand, the occurrence of higher harmonic components in the magnetoimpedance voltage has recently been detected and analysed in different GMI experiments [5, 11–14]. This occurrence is mainly ascribed to the intrinsic nonlinear magnetization process of the sample under the action of the circumferential magnetic field (H_ϕ) generated by the flow of the electrical ac current. Thus, its contribution can be reinforced through those experimental factors leading to a parallel enhancement of the nonlinear characteristics of the circular magnetization process (i.e. induction of a circumferential anisotropy and high ac current amplitude values in the GMI measurements). The very high dc field sensitivity of these nonlinear terms with respect to the fundamental response is very promising from the point of view of applications [15].

The occurrence of nonlinear terms in the GMI effect has therefore associated with it a nonlinear (variable) circumferential magnetic permeability, μ_ϕ. However, the classical electrodynamical model [16], extensively employed in the determination of the complex impedance Z, is based on the assumption of a constant value of μ_ϕ during the magnetization process. It has been shown that Fourier analysis can be suitably employed to obtain a mean value of μ_ϕ in any general case irrespective of the linear characteristics of the actual circumferential magnetization process [17, 18]. Using a simple rotational model to evaluate the circumferential magnetization (M_ϕ), the real and imaginary components of μ_ϕ can be directly obtained through the Fourier transformation of the time derivative of M_ϕ. Within this simple estimation procedure the main characteristics of the complex impedance have been suitably reproduced—that is, its axial field and current amplitude dependences and its evolution with the induction of circumferential anisotropy. With respect to the nonlinear terms, the estimation procedure described has shown the existence of a direct correlation between the second-harmonic term (V_{2f}) and the occurrence of asymmetrical characteristics in the circumferential magnetization process [17]. Such an asymmetry can be controlled by the induction of suitable magnetic anisotropies, that is, those associated with an increase of the skew angle of the easy axis with respect to the circumferential direction. Thus, the enhancement of the V_{2f} contribution is experimentally obtained through the application of tensile stress in positive magnetostriction samples [19] or the induction of helical anisotropies by the application of torsional strains [5, 20].

The aim of the present work is to analyse in further detail the torsional dependence of the nonlinear giant magnetoimpedance in a FeCoSiB amorphous wire. In particular, the axial field dependence of the complex impedance ($Z = R + \mathrm{i}X$) and the second-harmonic term (V_{2f}) are analysed as a function of the applied torsional strain. In order to enhance the nonlinear contribution the wire was initially subjected to current annealing (Joule heating) below the corresponding Curie point (induction of a circumferential anisotropy). The circumferential magnetization process is analysed in this work through the direct experimental determination of the low frequency circumferential hysteresis loops. The results directly confirm the validity of the Fourier analysis in the estimation of a mean value of the circumferential permeability.

Moreover, the correlation between the asymmetric circumferential magnetization process and the occurrence of nonlinear second-harmonic terms is directly confirmed.

2. Experimental details

The sample, an amorphous wire with nominal composition $(Co_{0.94}Fe_{0.06})_{72.5}Si_{12.5}B_{15}$, was initially obtained through the 'in-rotating-water-quenching' technique, with mean diameter 120 μm. A piece 8 cm in length was previously subjected to current annealing (Joule heating) with a current density $j = 24.3$ A mm^{-2} for 5 min. Since the Curie point corresponds to a current density of 32.1 A mm^{-2}, the induction of a circumferential anisotropy ($K_\phi = 19.9$ J m^{-3} [21]) takes place under the thermal treatment performed.

The magnetoimpedance effect was measured through the conventional four-probe technique, where the voltage drop across the sample and the current signal (obtained through a commercial current probe) were simultaneously recorded in a digital oscilloscope. Fourier analysis of the recorded magnetoimpedance voltage was employed to determine the first-harmonic (Z) and second-harmonic (V_{2f}) contributions. The experimental set-up allowed the application of a dc longitudinal magnetic field (long solenoid) and the simultaneous application of torsional stress, ξ, to the sample. In order to directly analyse the circumferential magnetization process of the sample, the circumferential hysteresis loops (M_ϕ–H_ϕ) were directly obtained in the same experimental configuration. The integration of the inductive voltage across the wire ends, once the resistive component was suitably subtracted through a Wheatstone bridge ($f = 800$ Hz), was employed to determine the circumferential magnetization of the sample.

3. Results

In order to check the occurrence of an initial torsional (helical) anisotropy within the sample, the zero-axial-field ($H = 0$) impedance was analysed as a function of the torsional strain (ξ). As is shown in [5], the unstrained state (ξ) is characterized by maximum values in both impedance components and a minimum contribution of the second-harmonic voltage (V_{2f}). Such a behaviour is found in the present experimental configuration for $\theta_i \approx -34°$ (anticlockwise torsional direction). Moreover, with respect to the driving frequency, the selected value ($f = 600$ kHz) promotes maximum magnetoimpedance ratios (maximum changes in the impedance values upon the application of the maximum axial applied magnetic field, $H \approx 400$ A m^{-1}).

Figures 1(a) and (b) show the axial field dependence of the resistance (R) and reactance (X), respectively, as functions of the applied torsional strain (ξ) for $I_0 = 10$ mA. The torsional strain values displayed are corrected taking into account the detected initial helical anisotropy, that is, $\xi(\pi \text{ rad m}^{-1}) = \frac{(\theta-\theta_i)\pi}{180L}$ (L: sample length). As previously reported [5, 7], the application of ξ should give rise to a decrease in both impedance components, as a result of the associated decrease of the circular permeability. Such behaviour can be clearly seen in figures 1(a) and (b), together with the occurrence of maximum values in both impedance components at certain values of the axial applied magnetic field (H_m). Table 1 summarizes the evolution of H_m with ξ obtained from $R(H)$ and $X(H)$ curves, where $\xi < 0$ and $\xi > 0$ represent, respectively, anticlockwise and clockwise applied torsional strains. In both cases, the application of ξ leads to an increase in H_m that would be associated with the reinforcement of the effective circumferential anisotropy [4, 8]. As regarding the maximum impedance values at H_m (Y_m), as the inset of figure 1 shows, both maximum impedance values present a continuous decrease with the application of ξ.

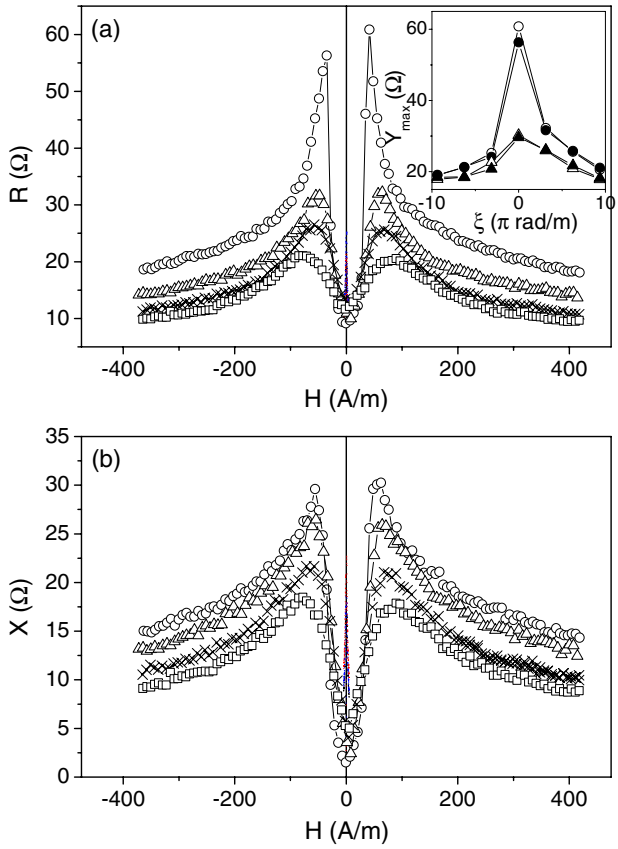

Figure 1. The axial field (H) dependence of the resistance R (a) and reactance X (b) for $I_0 = 10$ mA and $\xi = (\circ)$ 0, $(\triangle)$ 3.1, $(\times)$ 6.2 and $(\square)$ 9.4π rad m^{-1}. The inset of (a) shows the torsional (ξ) dependence of the maximum values of the impedance components, Y_m: R (circles) and X (triangles). The open and closed symbols correspond to positive and negative axial field values, H_m, respectively.

Table 1. Axial magnetic fields where maximum values of resistance and reactance components occur (H_{mR} and H_{mX}, respectively), as a function of the applied torsional strain, ξ.

ξ (π rad m^{-1})	H_{mR} (A m^{-1}) $I_{ac} = 10$ mA	H_{mX} (A m^{-1}) $I_{ac} = 10$ mA	H_{mR} (A m^{-1}) $I_{ac} = 50$ mA	H_{mX} (A m^{-1}) $I_{ac} = 50$ mA
−9.4	79.6	83.6	11.9	66.0
−6.2	79.6	80.4	10.3	73.2
−3.1	70.0	76.4	13.5	69.2
0	37.4	58.9	10.3	69.2
3.1	55.7	69.2	13.5	69.2
6.2	69.2	73.2	12.7	58.9
9.4	86.7	83.6	15.1	62.9

On the other hand, figures 2(a) and (b) show $R(H)$ and $X(H)$, respectively, as functions of ξ for $I_0 = 50$ mA. Surprisingly, the increase in the amplitude of the exciting current gives rise to a drastic decrease in the torsional strain sensitivity of Z. As shown in both table 1 and the inset of figure 2(a), H_m and the maximum values of both impedance components (Y_m) do

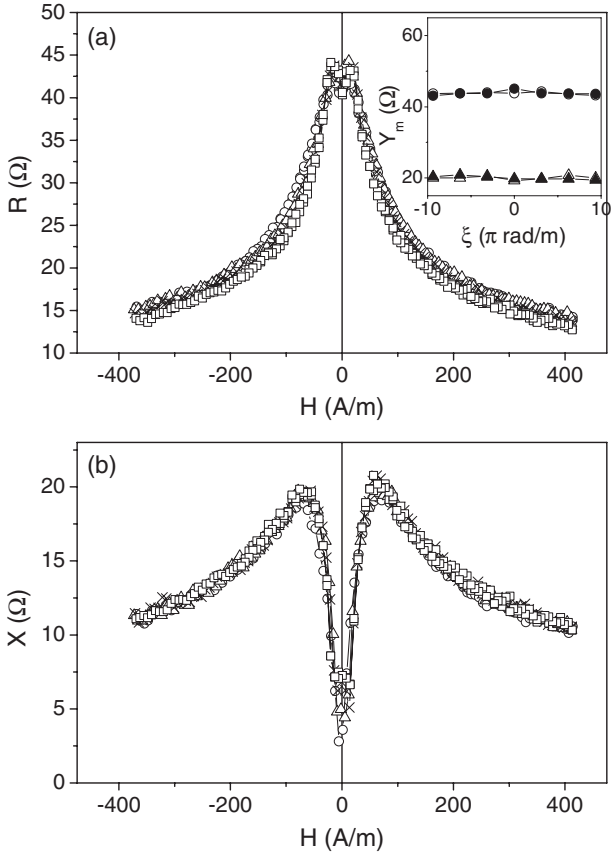

Figure 2. The axial field (H) dependence of the resistance R (a) and reactance X (b) for $I_0 = 50$ mA and $\xi = (\circ)$ 0, $(\triangle)$ 3.1, $(\times)$ 6.2 and $(\square)$ 9.4π rad m^{-1}. The inset of (a) shows the torsional (ξ) dependence of the maximum values of the impedance components, Y_m: R (circles) and X (triangles). The open and closed symbols correspond with positive and negative axial field values, H_m, respectively.

not significantly change upon the application of ξ. Moreover, H_m for the resistive component drastically decreases with respect to the evolution for $I_0 = 10$ mA. In this case ($I_0 = 50$ mA) R reaches its maximum values for $H \approx 10$ A m^{-1}.

With respect to the nonlinear response of the magnetoimpedance voltage, the axial field dependence of V_{2f} presents a very complex behaviour for low values of H (see figures 3(a) and (b), where $V_{2f}(H)$ is plotted for $I_0 = 10$ and 50 mA, respectively, for some selected ξ values). Also, the inset of figure 3(b) shows $V_{2f}(\xi)$ for an applied axial bias field $H = 159$ A m^{-1}. While for $I_0 = 50$ mA, V_{2f} displays a continuous increase with ξ, for $I_0 = 10$ mA, the occurrence of a maximum value is found for $\xi = \pm 3.1\pi$ rad m^{-1}.

In order to correlate the presented $Z(H, \xi)$ and V_{2f} (H, ξ) evolution with the actual circumferential magnetization process taking place within the sample, the circumferential hysteresis loops, M_ϕ–H_ϕ, were obtained with the same axial field and torsional strain experimental configuration. Figure 4 shows the low frequency (800 Hz) circumferential hysteresis loops (reduced circular magnetization $M_\phi/M_{\phi S}$, where $M_{\phi S}$ is the saturation magnetization, versus the estimated circumferential field at the wire surface ($H_\phi = I_0/2\pi a$,

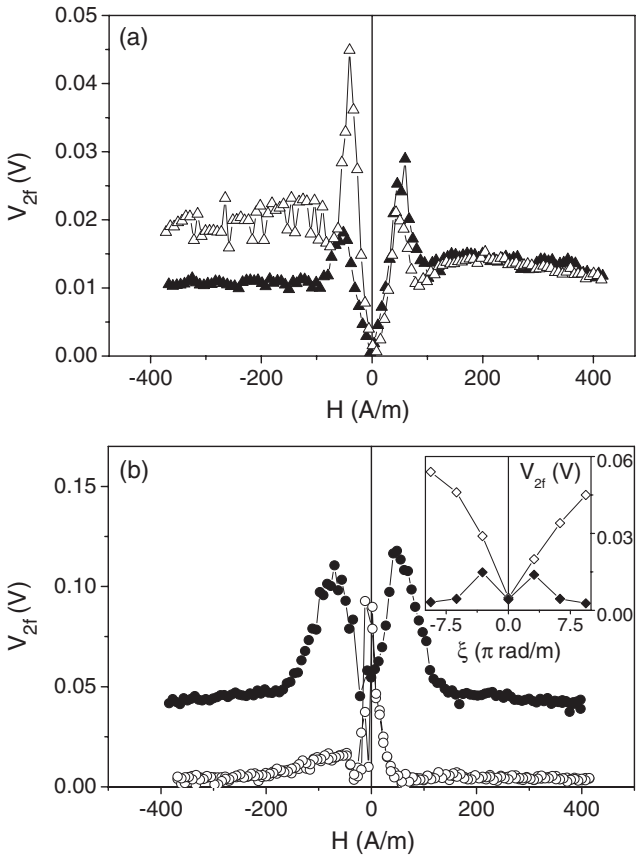

Figure 3. The axial field (H) dependence of the second-harmonic amplitude, V_{2f}: (a) $I_0 = 10$ mA and $\xi = (\triangle)\ 3.1\pi$ rad m^{-1} and $(\blacktriangle)\ -3.1\pi$ rad m^{-1}; (b) $I_0 = 50$ mA and $\xi = (\circ)\ 0$ and $(\bullet)\ -6.2\pi$ rad m^{-1}. Inset of (b): the torsional (ξ) dependence of the second-harmonic amplitude, V_{2f}, under a bias magnetic axial field of $H = 159$ A m^{-1} for $I_0 = (\blacklozenge)$ 10 and $(\diamond)$ 50 mA.

$I_0 = 50$ mA, a: wire radius)) at different axial magnetic fields for (a) $\xi = 0$ and (b) $\xi = -6.2\pi$ rad m^{-1}. For $H = 0$ and $\xi = 0$, a nearly rectangular hysteresis loop with two large Barkhausen jumps at $H_\phi \approx H_K$ ($H_K = \frac{2K_\phi}{\mu_0 M_S} \approx 50$ A m^{-1}; $\mu_0 M_S = 0.8$ T) are obtained. This result confirms the existence of a well-defined easy magnetic axis along the circumferential direction associated with the Joule heating performed. The application of an axial magnetic field results, for $H < H_K$, in a decrease in the associated circumferential coercive field, $H_{C,\phi}$ (increase in the effective circular magnetic permeability, μ_ϕ). A further increase in H leads to the disappearance of the irreversible Barkhausen jumps, and an almost reversible circumferential magnetization process (decrease in the effective value of μ_ϕ). With respect to the evolution of the torsional strained state (see figure 4(b)), the application of $\xi = -6.2\pi$ rad m^{-1} for $H = 0$ brings in a slight increase in $H_{C,\phi}$ (reinforcement of the effective circumferential anisotropy). While for $\xi = 0$ the sample exhibits a symmetrical circumferential magnetization process, irrespective of the value of H (see figure 4(a)), the application of H gives rise, in the strained state ($\xi = -6.2\pi$ rad m^{-1}), to a clear shift of the circumferential hysteresis loops towards positive H_ϕ values.

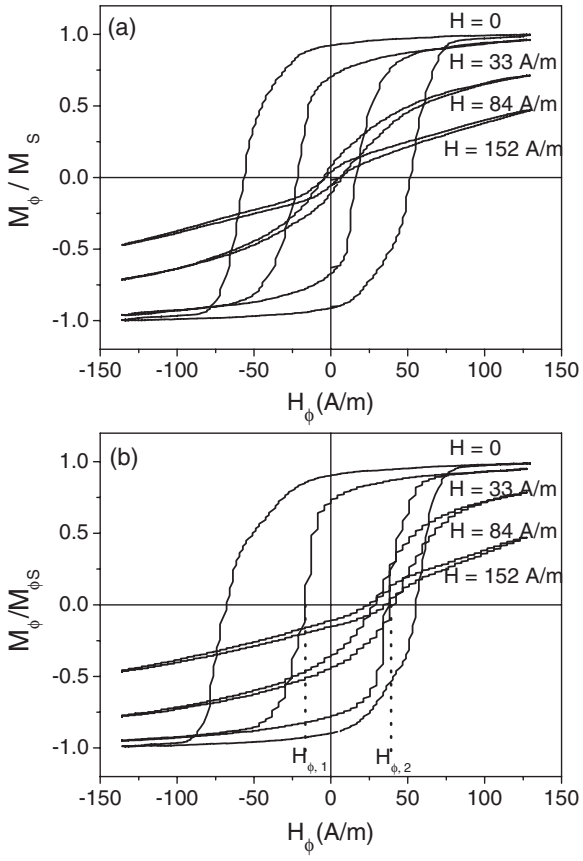

Figure 4. Circumferential hysteresis loops (reduced circular magnetization $M_\phi/M_{\phi S}$, where $M_{\phi S}$ is the saturation magnetization, versus the estimated surface circumferential field, $H_\phi = I_0/2\pi a$; a: wire radius) for (a) $\xi = 0$ and (b) $\xi = -6.2\pi$ rad m^{-1} at different values of the axial magnetic field.

4. Discussion

4.1. Axial field dependence of the complex impedance; estimation of the magnetic permeability

In previous works [17, 18], the axial field dependence of the impedance components has been analysed within a simple rotational model where the mean value of the circumferential magnetic permeability, μ_ϕ, is calculated through the Fourier analysis of the estimated $\partial M_\phi(t)/\partial t$. Thus, considering $H_\phi(t) = H_0 \cos(2\pi f t)$,

$$\begin{aligned} a_n &= \frac{2}{T}\int_0^T \frac{\partial M_\phi(t)}{\partial t}\cos(n2\pi f t)\,\mathrm{d}t; \\ b_n &= \frac{2}{T}\int_0^T \frac{\partial M_\phi(t)}{\partial t}\sin(n2\pi f t)\,\mathrm{d}t; \end{aligned} \tag{1}$$

the mean value of the circumferential magnetic permeability can be expressed as $\mu_\phi = \mu_0 C(-b_1 + \mathrm{i}a_1)$, with $C = \frac{1}{2\pi f H_0}$ ($n = 1$ in equation (1)). This simple estimation, together

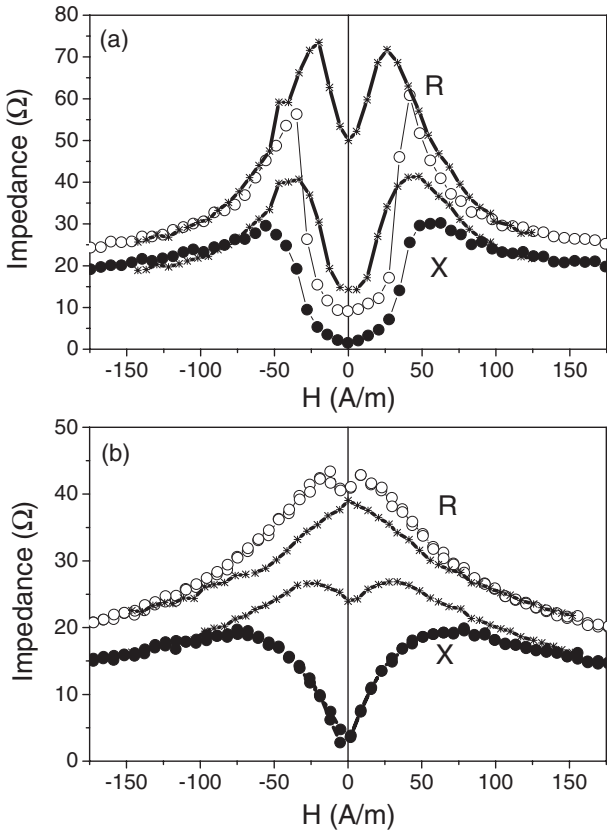

Figure 5. The axial field (H) dependence of the (●) resistance, R, and (○) reactance, X, for (a) $I_0 = 10$ mA and (b) $I_0 = 50$ mA. The solid curve (——) represents the estimated evolution.

with the classical electrodynamical theory [16], allows the determination of the impedance Z:

$$Z = \frac{1}{2} R_{\mathrm{dc}} ka \frac{J_0(ka)}{J_1(ka)} \tag{2}$$

with $R_{\mathrm{dc}} = \frac{\rho L}{\pi a^2}$ (ρ: electrical resistivity; L: effective sample length), $k = \sqrt{\frac{\mathrm{i}2\pi\mu_\phi f}{\rho}}$ and J_i the Bessel functions of the first kind.

In the present work a different approach is presented through the direct experimental determination of the circumferential magnetization process (M_ϕ–H_ϕ circumferential hysteresis loops). Introducing the experimental $\partial M_\phi(t)/\partial t$ in equation (1), the mean value of μ_ϕ and the complex impedance are directly estimated (equation (2)). Figures 5(a) and (b) show the comparison between the experimental (symbols) and the estimated (solid curve plus $*$) impedance values for $I_0 = 10$ and 50 mA, respectively. It is worth noting that each asterisk on the estimated curves of figures 5(a) and (b) represents an impedance value obtained from the experimental circumferential hysteresis loops and the previously described estimation procedure. As shown in figure 5, the estimated curves roughly describe the main characteristics of the experimental axial field dependence of the impedance components:

(i) the occurrence of a maximum value of X at $H \approx H_K = 50$ A m^{-1} for $I_0 = 10$ mA;
(ii) the decrease of H_{m} with the amplitude of the exciting current, I_0;
(iii) the parallel decrease in both impedance components with I_0.

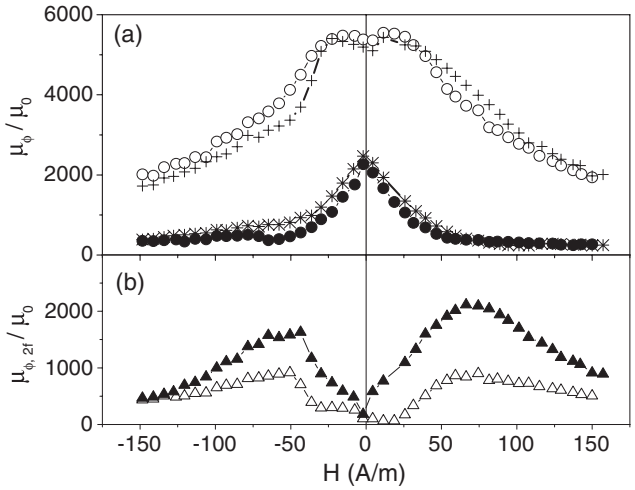

Figure 6. (a) The axial field (H) dependence of the real ($\mu_{\phi,\mathrm{r}}$) and imaginary ($\mu_{\phi,\mathrm{i}}$) components of the circular permeability: (○) $\mu_{\phi,\mathrm{r}}$ and (●) $\mu_{\phi,\mathrm{i}}$ for $\xi = 0$, (+) $\mu_{\phi,\mathrm{r}}$ and (*) $\mu_{\phi,\mathrm{i}}$ for $\xi = -6.2\pi$ rad m^{-1}; (b) the dependence of the second-harmonic component of the magnetic permeability, $\mu_{\phi,2f}$, on the axial magnetic field (H) for (△) $\xi = 0$ and (▲) $\xi = -6.2\pi$ rad m^{-1}.

It is worth remarking on the excellent agreement, irrespective of the actual value of I_0, between the experimental and estimated curves for high axial magnetic fields where the rotational contribution dominates the circumferential magnetization process (see figure 4). However, the estimated curves separate from the experimental data for low values of H, where the domain wall movements mainly contribute at low frequencies. In this low axial field regime, the estimated permeability obtained from the circumferential hysteresis loops ($f = 800$ Hz) overcomes the actual values acting on the GMI measurements at higher frequency (600 kHz). Therefore, the occurrence of domain wall relaxation phenomena at high values of f gives rise to a decrease in the permeability values, and therefore to a parallel decrease in the experimental impedance data when compared with the estimated evolution derived from the low frequency hysteresis loops.

As regards the torsional dependence of the magnetoimpedance voltage, figure 6(a) shows the axial field dependence of the estimated permeability components ($\mu_\phi = \mu_{\phi,\mathrm{r}} - \mathrm{i}\mu_{\phi,\mathrm{i}}$) obtained for $\xi = 0$ and -6.2π rad m^{-1} ($I_0 = 50$ mA) from the experimental circumferential M_ϕ–H_ϕ loops. As expected (see figure 2), the application of ξ slightly changes the permeability components. However, a small decrease in $\mu_{\phi,\mathrm{r}}$ and an increase in $\mu_{\phi,\mathrm{i}}$ with ξ are detected, associated with a parallel increase in the circumferential coercivity of the sample (see figure 7 where $H_{\mathrm{C},\phi}(H)$ is plotted for $\xi = 0$ and -6.2π rad m^{-1}). This smooth torsional dependence could be interpreted as a direct consequence of the low strength of the induced magnetoelastic anisotropy (i.e. small value of the magnetostriction constant of the sample, $\lambda_{\mathrm{S}} \approx 10^{-8}$ [21]). On the other hand, as figure 1 shows, for $I_0 = 10$ mA both impedance components drastically change with ξ. Notice that the highest torsional sensitivity is obtained in the axial field region where the mean circumferential field lies below the circumferential coercivity of the sample (the maximum circumferential field at the wire surface, $H_{\phi,\mathrm{m}} = 26.5$ A m^{-1} for $I_0 = 10$ mA). In this initial permeability region where $H_{\phi,\mathrm{m}} < H_{\mathrm{C},\phi}$, the application of ξ promotes sharp changes in Z in spite of the low magnetostriction of the sample. For high enough axial magnetic fields, where the magnetization process takes place by reversible rotations, $H_{\phi,\mathrm{m}} > H_{\mathrm{C},\phi}$ and again the torsional sensitivity of the impedance components is drastically reduced.

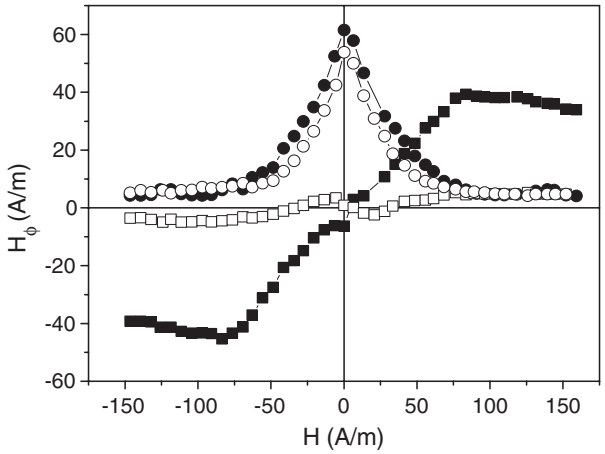

Figure 7. The circumferential coercive field, $H_{\phi,\mathrm{C}}$ ((○) $\xi = 0$ and (●) $\xi = -6.2\pi$ rad m^{-1}), and 'shift' circular field, $H_{\phi,\mathrm{S}}$ ((□) $\xi = 0$ and (■) $\xi = -6.2\pi$ rad m^{-1}), as a function of the axial magnetic field.

4.2. The nonlinear second-harmonic term

Let us now discuss the occurrence of a second-harmonic contribution in the magnetoimpedance voltage. It has been demonstrated that its origin can be mainly correlated with the existence of an asymmetrical circumferential magnetization process [5, 17, 20]. In fact, this is the basis of the detection method in highly sensitive flux-gate magnetic sensors [22], where the application of a dc magnetic field to a high permeability material introduces an asymmetry in the axial magnetization process. In the case of the nonlinear magnetoimpedance, it has been found that the experimental second-harmonic component (V_{2f}) of the magnetoimpedance voltage can be basically described by the second-harmonic contribution of the magnetic permeability, $\mu_{\phi,2f}$ ($n = 2$ in equation (2)), obtained from the estimation procedure described [17]. Nevertheless, a direct correlation between V_{2f} and $\mu_{\phi,2f}$ in a general case, where the skin effect dominates the magnetoimpedance voltage, cannot be directly obtained through the classical electrodynamical model by a direct substitution of $\mu_{\phi,2f}$ into equation (2) (notice that this impedance expression is strictly valid in the particular case where μ_ϕ is strictly constant and linear with respect to the exciting circumferential field).

Taking into account the above described limitations, figure 6(b) shows the axial field dependence of the estimated $\mu_{\phi,2f} = C\sqrt{a_2^2 + b_2^2}$ ($n = 2$ in equation (1)) obtained in the present case through the experimental M_ϕ–H_ϕ hysteresis loops. As shown in figure 3(b), $\mu_{\phi,2f}(H)$ roughly describes the experimental $V_{2f}(H)$ and its evolution with the application of $\xi = -6.2\pi$ rad m^{-1}. Hence, the reinforcement of V_{2f} with ξ, the occurrence of maximum values for $H \approx H_K$ and the existence of a certain asymmetry in the peak value of V_{2f} for positive and negative H values are qualitatively well described by the model.

However, as previously stated, $V_{2f}(H, \xi)$ and thus $\mu_{\phi,2f}(H, \xi)$ are directly correlated with the asymmetrical characteristics of the circumferential magnetization process. In order to reinforce such a correlation, the shift of the circumferential hysteresis loops was analysed through the definition of the displacement circumferential field, $H_{\phi,\mathrm{S}} = (H_{\phi,2} - H_{\phi,1})/2$ (see figure 4(b)). As shown in figure 7, where $H_{\phi,\mathrm{S}}(H)$ is plotted for $\xi = 0$ and -6.2π rad m^{-1}, the displacement of the circumferential hysteresis loops is almost negligible in the unstrained state ($\xi = 0$). This symmetrical circumferential magnetization process is associated (see

figure 3(b)) with nearly null values of V_{2f}. However, the occurrence of non-zero values of V_{2f} around $H \approx 0$, which cannot be satisfactorily explained in terms of $H_{\phi,S}$ and $\mu_{\phi,2f}$ (see figures 7 and 6(b), respectively), is remarkable. This result could be linked to the fact that, when the skin effect dominates the magnetoimpedance response, the classical electrodynamical model should be modified to take into account the occurrence of nonlinear permeability terms, where the contribution of domain wall movements should also be considered. However, for $\xi = -6.2\pi$ rad m^{-1} a direct relationship between $H_{\phi,S}(H)$ and $V_{2f}(H)$ is found, i.e. the parallel increase with ξ and the occurrence of maximum values at axial field values around the anisotropy field. Also, the final sharp decrease of V_{2f} for $H > H_K$ (also displayed by $V_{2f}(H)$ for $I_0 = 10$ mA; see figure 3(a)) should be mainly ascribed, as shown by the circumferential hysteresis loops (see figure 4(b)), to a parallel reduction in M_ϕ instead of a drastic reduction of the asymmetry in the circumferential magnetization process.

5. Conclusions

The axial field dependence of the impedance ($f = 600$ kHz) and its evolution with the applied torsional strain (ξ) is analysed in a Joule heated $(Co_{0.94}Fe_{0.06})_{72.5}Si_{12.5}B_{15}$ amorphous wire. In spite of the low sample magnetostriction ($\approx 10^{-8}$), high torsional sensitivities are found for low values of the current amplitude. Moreover, the behaviour of the second-harmonic component is also analysed, and its axial field dependence studied in terms of the effect of the induced helical magnetoelastic anisotropy. These results are interpreted through the analysis of the corresponding changes taking place in the circumferential magnetization process (experimental circumferential hysteresis loops at 800 Hz). In particular, the mean values of the magnetic permeability and its nonlinear (second-harmonic) terms are obtained through the Fourier analysis of the time derivative of the experimental circumferential magnetization. The results clearly confirm the enhancement of the second-harmonic contribution of the magnetoimpedance voltage through the reinforcement of the asymmetric characteristics of the circumferential magnetization process (i.e. induction of the helical magnetoelastic anisotropy).

Acknowledgments

JGSD and MK acknowledge FAPESP and CNPq (Brazilian agencies) for their financial support. The work was partially supported by the Spanish 'Gobierno de Navarra' under project 'Propiedades de magnetotransporte de nuevos materiales nanoestructurados'.

References

[1] Panina L V, Mohri K, Bushida K and Noda M 1994 *J. Appl. Phys.* **76** 61
[2] Mohri K, Shen L P, Cai C M, Panina L V, Honkura Y and Yamamoto M 2002 *IEEE Trans. Magn.* **38** 3063
[3] Knobel M, Kraus L and Vázquez M 2003 *Handbook of Magnetism and Magnetic Materials* vol 15, ed K H J Buschow (New York: Elsevier) p 497
[4] Blanco J M, Zhukov A and Gonzalez J 2000 *J. Appl. Phys.* **87** 4813
[5] Losin C, Gómez-Polo C, Knobel M and Grishin A 2002 *IEEE Trans. Magn.* **38** 3087
[6] Hernando B, Prida V M, Sánchez M L, Gorría P, Kurlyandkaya G V, Tejedor M and Vázquez M 2003 *J. Magn. Magn. Mater.* **258/259** 183
[7] Li Y F, Vázquez M and Chen D X 2003 *J. Appl. Phys.* **93** 9839
[8] Betancourt I and Valenzuela R 2003 *Appl. Phys. Lett.* **83** 2022
[9] Panina L V 2002 *J. Magn. Magn. Mater.* **249** 278
[10] Mohri K, Uchiyama T, Shen L P, Cai C M, Panina L V, Honkura Y and Yamamoto M 2002 *IEEE Trans. Magn.* **38** 3063
[11] Gómez-Polo C, Vázquez M and Knobel M 2001 *J. Magn. Magn. Mater.* **226–230** 712

[12] Kurlyandskaya G V, Yakabchuk H, Kisker E, Bebenin N G, García-Miquel H, Vázquez M and Vas'kovskiy V O 2001 *J. Appl. Phys.* **90** 6280
[13] Antonov A S, Buznikov N A, Granovsky A B, Iakubov I T, Prokoshin A F, Rakhmanov A L and Yanukin A M 2002 *J. Magn. Magn. Mater.* **249** 315
[14] Duque J G S, de Araujo A E P, Knobel M, Yelon A and Cireanu P 2003 *Appl. Phys. Lett.* **83** 99
[15] Kurlyandskaya G V, García-Arribas A and Barandiarán J M 2003 *Sensors Actuators* A **106** 234
[16] Landau L D, Lifschitz E M and Pitaevski L P 1995 *Electrodynamics of Continuous Media* (London: Butterworth-Heinemann) p 212
[17] Gómez-Polo C, Knobel M, Pirota K R and Vázquez M 2001 *Physica* B **299** 322
[18] Gómez-Polo C, Vázquez M and Knobel M 2001 *Appl. Phys. Lett.* **78** 322
[19] Gómez-Polo C, Pirota K R and Knobel M 2002 *J. Magn. Magn. Mater.* **242–245** 294
[20] Duque J G S, Gómez-Polo C, Yelon A, Cireanu P, de Araujo A E P and Knobel M 1994 *J. Magn. Magn. Mater.* **271** 390
[21] Gómez-Polo C and Vázquez M 1993 *J. Magn. Magn. Mater.* **118** 86
[22] Borhöfft W and Trenkeler G 1989 *Sensors: a Comprehensive Survey* vol 5 (New York: VCH) p 153